An overview of flux braiding experiments

A.L. Wilmot-Smith

Division of Mathematics, University of Dundee, Dundee, DD1 4HN.

Abstract

Parker has hypothesised that, in a perfectly ideal environment, complex photospheric motions acting on a continuous magnetic field will result in the formation of tangential discontinuities corresponding to singular currents. We review direct numerical simulations of the problem and find the evidence points to a tendency for thin but finite thickness current layers to form, with thickness exponentially decreasing in time. Given a finite resistivity these layers will eventually become important and cause the dynamical process of energy release. Accordingly, a body of work focusses on evolution under continual boundary driving. The coronal volume evolves into a highly dynamic but statistically steady state where quantities have a temporally and spatially intermittent nature and where the Poynting flux and dissipation are decoupled on short timescales. Although magnetic braiding is found to be a promising coronal heating mechanism much work remains to determine its true viability. Some suggestions for future study are offered.

1 Introduction

The notion that solar coronal loops are heated as an end result of magnetic braiding dates back to the 1970s and Parker's notion of topological dissipation [1, 2, 3]. The hypothesis is built on the foundation that the solar corona can be modelled as a largely force-free environment, with the Lorentz forces in force balance. However, loops themselves are subject to photospheric motions at their footpoint and hence slow footpoint motions will lead to the quasi-static evolution of loops through sequences of force-free equilibria. Complex footpoint motions applied to the base of a coronal loop will twist and tangle the magnetic field which must then relax to a force-free state. Given the extremely high Lundquist numbers of the corona the relaxation will be ideal and so will preserve exactly the magnetic field topology.



Figure 1: Evolution of an M-class solar flare observed by the *Transition Region and Coronal Explorer* at 06:34UT, 08:13UT and 09:03UT on 14th September 2000 in the 171Å passband. An apparently tangled magnetic field structure relaxes to a simpler configuration after the flare.

The question is then whether a magnetic field of arbitrary topology can relax ideally to a smooth force-free equilibrium. Parker hypothesised that the space of force-free fields is restricted, so that smooth equilibria will not generally exist and, instead, the magnetic field will develop tangential discontinuities corresponding to current sheets [1]. Of course in a real corona as soon as sufficiently small length scales develop then diffusion will locally become appreciable and a change in the magnetic topology can occur, releasing energy. This release of magnetic energy, built up through braiding, could, under the Parker hypothesis, explain the observed high temperatures of coronal loops.

Observing braided magnetic fields in the corona has so far been fraught with difficulty. Although a very few observations (such as those of Figure 1) suggest large-scale magnetic fields can have braided configurations, most observations of coronal loops show an apparently well-combed structure. The latest high-resolution images from Hi-C are more suggestive of braids [4], although how the apparently crossing structures relate to the underlying magnetic field is not immediately clear [5]. A non-linear force-free extrapolation of the region [6] does suggest a complex structure. Although the extrapolated magnetic field outlines the crossings seen in the observations, it is also constructed from lower-resolution magnetograms. Furthermore, the flux tube determined is split along its length which can only be the result of at least one coronal null point. A null point in such a coronal volume is expected from our current understanding of the structure of coronal fields: they are known to be permeated by nulls, separatrix surfaces and separators [7]. A review in this volume [8] discusses the significance of heating at these features, which was already acknowledged by Parker: "Insofar as the field is concentrated into separate individual magnetic fibrils at the photosphere, each individual fibril moves independently of its neighbors, producing tangential discontinuities (current sheets) ... There is, however,

a more basic effect, viz., a continuous mapping of the footpoints spontaneously produces tangential discontinuities" [2]. Accordingly, braiding as discussed in this review refers specifically to the elementary effect in individual elemental loops. These loops are not resolved by current instruments and, given their aspect ratio, fine scale braiding within a loop would likely appear smoothed out.

The notion of footpoint motions acting on the complex coronal field with all of its topological features has been formalised into the theory of coronal tectonics [9]. Simulations addressing this relevant scenario are so far rare, with just a very few examining the basic effect [10, 11, 12, 13]. One important series of articles implicitly fall into this framework [14, 15, 16, 17]. Here a potential magnetic field is extrapolated into the corona from a smoothed active region magnetogram and a convection-like driving velocity applied to its simulated photospheric boundary. Although the resolution of these large-scale simulations is not sufficient to provide an understanding of exactly where or how the dissipation is occurring, the broad comparisons to observed loops are encouraging.

An understanding of the viability of the Parker mechanism for coronal heating requires an two-pronged attack both by theory and by direct numerical simulation, while this review discusses only the latter approach. As we will detail in Section 2, numerical evidence does not, at least to date, demonstrate the ubiquitous formation of singular current sheets. Nevertheless, simulations all agree that small scales in the current do rapidly develop under generic braiding conditions and these will eventually become small enough to initiate dissipation. Hence a second main question to be tackled by braiding simulations arises: given a finite resistivity, how does the coronal magnetic field evolve when it is continuously driven by photospheric motions? A discussion of the main simulations tackling these various questions is given in Section 2, presented in four broad classes according to simulation setup. Conclusions are briefly drawn in Section 3 together with an outline of some suggestions for future work.

2 Braiding Simulations

Numerical simulations of flux braiding naturally divide into four categories. These are not all distinct, with some simulations falling into more than one category. Nevertheless the division is helpful to describe the present state of knowledge. In brief, the groups of simulations are:

(a) Sequences of shears. A loop is subjected to a sequence of simple shearing motions on the boundary.

- (b) Continually driven systems. A loop is subjected to boundary motions, generally of rotational form, for an extended period of time.
- (c) Formation of discontinuities. The question of whether or not tangential discontinuities form in a coronal volume subjected to boundary motion is examined by simulation.
- (d) *Initially braided fields*. The coronal volume is not braided self-consistently via boundary motions but a braided magnetic field is taken as an initial condition for a simulation.

Each of the simulations discussed in this review have a broadly similar experimental setup. To model the coronal loop the magnetic field is straightened out to lie between two parallel plates. Hence a Cartesian geometry is employed and in the numerical box both the upper and lower boundaries represent the photosphere. A velocity field imposed on one or both boundaries represents a photospheric flow. The flow is two–dimensional and flux emergence (or cancellation) is not considered. We detail results found for simulations in each of the classes given above in the following sections, beginning with the earliest form of simulation, that of boundary shear.

2.1 Sequences of boundary shears

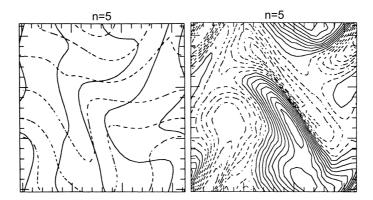


Figure 2: Illustrating the nature of the force-free equilibria attained by van Ballegooijen [19] following 5 boundary shearing motions applied to an initially homogeneous field. Displacement of fluid elements on the upper boundary (*left*) and vertical component of the electric current near the lower boundary (*right*). Image adapted from [19].

Table 1 provides a short summary of simulation setups where initially uniform magnetic fields are subjected to shearing motions on their boundaries. Here, and throughout this

Table 1: Outline of braiding simulation setups investigating evolution when shearing

motions are applied to loops.

Article	Evolution	Grid		Box	Driver properties
	Method	size		size	1 1
van Ballegooijen [18, 19]	magnetic energy minimisa- tion	N/A		13	Upper boundary only: sequence of 5 low amplitude perpendicular shears with random phase angle
Mikić, Schnack, van Hoven [20]	Simplified 3D ideal MHD	64^{3}		13	Lower boundary only: 12 low amplitude perpendicular flows based on [18, 19]
Longbottom et al. [21]	magneto- frictional	$ up $ $ 65^3 $	to	1 ³	Fixed high amplitude initial shear, second perpendicular shear of varying amplitude.
Galsgaard & Nordlund [22]	3D resistive MHD	up 136 ³	to	1^3 or $1^2 \times 10$	Both boundaries driven, random amplitudes, phases and durations.
Bowness et al. [23]	3D ideal/ resistive MHD	512 ³		$1^2 \times 4/3$	Two perpendicular shears (second switches off in one study, continues in another).

section, the term shearing flow is used to describe one running on opposite directions on either side of a neutral flow line. Van Ballegooijen [18, 19] was the first to describe such a simulation, applying a shearing flow on the lower boundary of the domain in an alternating sequence of perpendicular directions (\mathbf{e}_y , \mathbf{e}_x , \mathbf{e}_y , etc.) with differing, randomly chosen, phase angles. The flow amplitude and duration were each chosen such that the maximum displacement of fluid elements on the boundary is around 16% of the domain size. The mapping of magnetic field lines from lower to upper boundary is shown to develop fine scales in the evolution, with the scales decreasing exponentially with number of shear events [18]. Although this work was developed before the concept of the quasi-separatrix layer (QSL) was developed [24], the idea is essentially the same: QSLs in the domain have a thickness exponentially decreasing in time. Fluid displacements on the upper boundary after 5 shears are shown in the left-hand image of Figure 2.

The corresponding volume force-free magnetic field was obtained following each boundary displacement using an energy minimisation iterative procedure on a 32^3 numerical grid [19]. Using this approach a total of five shears were successfully applied before the method itself failed. While it is not a priori clear that the existence of small scales in the magnetic field line mapping also forces the magnetic field and current to have the

same small scales, this does turn out to be the case in the example presented [19]. Hence the length scales of the current also exponentially decrease with number of shears. The current structure after 5 shears is shown in the right-hand image of Figure 2.

Mikić, Schnack & van Hoven [20] took a similar approach, again applying a shear sequence to the lower boundary of a unit cube containing a magnetic field. Their numerical scheme, a simplification of the ideal MHD equations that neglects the inertial term and employs a high viscosity, allows for a successive sequence of 12 force-free relaxations on a 64³ grid to be calculated. The main findings of van Ballegooijen [18, 19] were confirmed, with the cascade to smaller scales giving an exponential growth in current density but with a smooth force-free equilibrium achieved in each step. A consequence of the exponential decrease in current layer thickness with shear is that a tangential discontinuity will only be reached after an infinite time. However, in practice current densities will be strong enough to become dynamically important in a plasma of finite resistivity.

While the shears applied in [18, 19, 20] all have a low amplitude (< 20% of the domain size), Longbottom et al. [21] considered the question of how the shear amplitude itself (rather than number of shears) might affect the field evolution. The authors employed an ideal magnetofrictional relaxation method [25], and applied shearing motions on both the upper and lower boundaries of the domain. The initially uniform magnetic field on the unit cube was first subjected to a shear of amplitude 0.8 (as a fraction of the domain size) and then relaxed to a force-free state that was found to be smooth. This state was taken as an initial condition for a parameter study in which a perpendicular shear of various strengths was applied before relaxation. The amplitude of the second shear is shown to be crucial in determining the nature of the final force-free state. In all cases a twisted current structure is found running through the domain. The basic structure of the twisted current layer was confirmed by Bowness et al. [23] who imposed analytically an initial shear and then used an ideal 3D MHD code at 512³ to evolve the magnetic field through a second, perpendicular, shear event. Taking a second shear strength of 0.5 a twisted current layer forms (Figure 11(a) and Figure 14 of [23]) running through the domain, agreeing with [21].

The width of the current layer depends on shear strength [21]: for low shear values (below 0.5) the layer is well resolved while for high shear (above 0.6) its behaviour is consistent with that of a true tangential discontinuity. That is, the maximum current in the layer increases linearly or faster as the grid resolution is increased (power law growth is expected for a true current sheet [26]). The simulation of Longbottom et al. [21] marks the first (and essentially only) demonstration of a case that is consistent with Parker scenario of topological dissipation [1]. With the resolution available at that time

(a Lagrangian grid of maximum size 65^3) and known inaccuracies in the scheme for high grid deformation [27], the possibility remains that the growth of maximum current with resolution in the high shear cases could level off at higher resolutions. An increase in grid size has only very recently become accessible [28] and this possibility is, as-yet, untested. Under either of these aforementioned scenarios (an exponential decrease in current thickness or the formation of singular current layers in ideal MHD) in a real physical plasma the resistivity will at some point become important. To determine the consequences of a finite resistivity, Galsgaard & Nordlund [22] employed a fully resistive 3D MHD simulation to examine behaviour of a coronal loop continually subjected to boundary shearing motions. The authors detail an extensive set of simulations, common to all of which is the application of perpendicular shears of random amplitude, phase and duration to both the upper and lower boundaries of the model loop. Runs consider the effect of driver speed (0.02-0.4 compared with the Alfvén speed of 1) and duration, loop aspect ratio, and grid resolution (24^3-136^3) , with all runs extending for many Alfvén loop crossing times.

Some results are common to each of the simulations in [22]: shearing motions cause a rapid growth in the electric current (with maximum strength increasing exponentially in the early phase), dissipation becomes important and within two or three shears a statistically steady state is reached where quantities (including the maximum current and total magnetic energy) fluctuate about an average level. In such steady states the current structure is fragmented with Joule dissipation taking place over a wide range of scales. Figure 3 shows isosurfaces of current in one particular run. Dissipation has an increasingly bursty character for the higher box aspect ratio cases. The magnetic field structure (some example field lines are shown in Figure 3) is generally complex, including reversals in the field component perpendicular to the driven boundaries. No significant twist is built up in the system but magnetic energy in excess of potential in the steady states varies significantly. The key factor appears to be the boundary driving velocity: for the 1:10 aspect ratio loop the mean energy in excess of potential in the statistically steady states is just 1.5% for the slower driver of at a 0.02 fraction of the Alfvén velocity but 45% for the faster driver at a 0.2 fraction of the Alfvén velocity. The simulation series of Galsgaard & Nordlund [22] is one in a wider class of simula-

The simulation series of Galsgaard & Nordlund [22] is one in a wider class of simulations in which a coronal volume is continually driven under a resistive evolution. Such simulations are the subject of the next section.

Table 2: Outline of braiding simulation setups investigating continually driven coronal

loops.

Article	MHD evo- Grid size		Box size	Driver properties
Longcope & Sudan [29]	lution type reduced	$16^2 \times 10$ to $48^2 \times 10$	1^3	Time-dependent rotational cells, both boundaries, 20–150 crossing times.
Galsgaard & Nordlund [22]	resistive 3D	up to 136 ³	1^3 and $1^2 \times 10$	Time dependent shear sequences, both boundaries, typically ~ 30 crossing times.
Hendrix & van Hoven [30]	simplified 3D	$32^2 \times 31$ to $256^2 \times$ 31	$(2\pi)^2 \times 8\pi$	Time-dependent rotational cells, both boundaries, 600 crossing times.
Gomez <i>et al.</i> [31]	reduced	$192^2 \times 32,$ $384^2 \times 32$	$(2\pi)^2 \times 10$	Stationary rotational cells, upper boundary, ~ 100 crossing times.
Rappazzo et al. [32, 33, 34, 35]	reduced	typically $512^2 \times 200$	$1^2 \times 10$	 Stationary rotational cells, both boundaries, ~ 600 crossing times [32, 33]. Comparison cases: uniform shear [34], uniform single localised vortex [35].
Ng <i>et al.</i> [36]	reduced	$64^2 \times 16$ to $512^2 \times$ 64	1^3	Time-dependent rotational cells (as [29]), both boundaries, 10000 crossing times.
Dahlburg et al. [37]	resistive (with con- duction, radiation)	128^{3}	$1^2 \times 5$	Time-dependent rotational cells, both boundaries, 700 crossing times.
Bowness et al. [23]	ideal and resistive 3D	512 ³	$1^2 \times \frac{4}{3}$	Two perpendicular shears, second shear indefinite or stops, both boundaries, 25 crossing times.

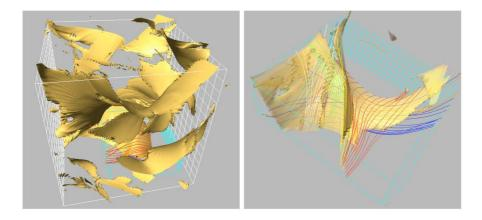


Figure 3: Instantaneous isosurfaces of current at a representative time in a simulation where a loop is continually driven by shearing boundary motions [22]. The left-hand image shows the full domain (boundary driving surfaces indicated with a grid) and the right-hand image a sub-section (the blue box of the left-hand image). The current has a fully three dimensional and space-filling structure. Image reproduced with permission from [22].

2.2 Continually driven systems

An outline of the continually driven simulations discussed here is given in Table 2. Strong currents rapidly build up in these systems and so in general resistive schemes are required to consider the longer-term evolution. The schemes taken vary but a frequent choice, largely for reasons of computational efficiency, is to follow the evolution in a (resistive) reduced MHD (RMHD) scheme [38, 39, 40]. Under the RMHD assumption an ordering to the system is assumed. The axial magnetic field component $B_0\mathbf{e}_z$ remains constant while the perpendicular component b varies in space and time (its vector potential is evolved) and is such that $|\mathbf{b}|/B_0 \approx \epsilon \ll 1$. The velocity field is forced to be incompressible and of order ϵ and the result is a nonlinear system of two equations that evolve the vorticity and the magnetic vector potential. The current itself is only in the vertical \mathbf{e}_z direction (but depends on all three coordinates). There is typically no energy equation in an RMHD evolution so that heat from any dissipation in the system is immediately drained away. Of the continually driven systems outlined in Table 2, two [22, 23] are shearing experiments and have been described in Section 2.1. The remaining works [29, 30, 31, 32, 33, 36, 37] have footpoint motions that are broadly similar, all being modelled on incompressible projections of convection. The convection of solar granulation is naturally compressible and allows for flux emergence and cancellation. Braiding simulations exclude these phenomena and so motivate the use of rotational cellular footpoint motions

in simulations (an incompressible model for convection). Examples of such footpoint motions are illustrated in Figure 4. Note that Longcope & Sudan [29] and Ng et al. [36] both use the same driver which is time-dependent and derived from a source of stationary random noise (illustrated at one particular time in Figure 4, second from left).

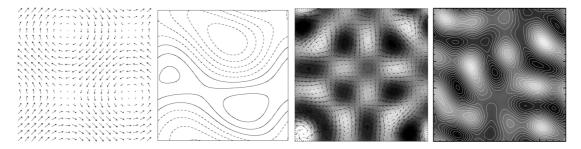


Figure 4: Streamlines and vector fields at particular times of the boundary driving velocities applied to coronal loops in various continually driven simulations. Left [30] (particular frame from time-dependent simulation); second from left is a frame from the time-dependent driver of [29] and [36] (reproduced with permission from [41]), second from right [31] (stationary driver) and right [32, 33] (stationary driver adapted from [33]).

In addition to the rotational drivers, Rappazzo et al. ([34, 35]) present two comparison cases. These are stationary drivers, one with a constant shearing profile [34] and the other a localised single vortex motion [35]. The motivation for these simple drivers would initially be to produce instabilities (tearing mode and kink instabilities respectively) rather than as relevant profiles for field line braiding. We include these cases here to motivate a discussion of how the driver itself affects evolution.

Several features are common to each of the systems described in this section. The most fundamental feature is that after a fairly short time statistically steady states are reached where quantities (e.g. total magnetic and kinetic energies, dissipation) fluctuate in time about an average level. The average levels as well as the character of the intermittency both depend on the simulation details. Figure 5 shows the volume magnetic and kinetic energies in time for particular runs from [36] and [32, 33]. In these and other cases magnetic energy dominates significantly over kinetic energy (example ratios 10: 1 [29], 40:1 [36, 32, 33], 80:1 [23]). Rappazzo et al. [32] find the power spectrum of the total energy depends on the typical driving velocity compared with the Alfvén speed, steepening as the driving velocity is comparably increased (in common with [22]).

Ng et al. [36] show that the average free magnetic energy levels increases with magnetic Reynolds number (Figure 5, left). Noteworthy for comparison is that for the continually applied stationary shearing profile of Rappazzo et al. [34] a significant amount of

magnetic energy initially builds up until a tearing-mode-like instability occurs. At that point a sizeable proportion of the free energy is released but further driving leads only to a statistically steady state and no further significant free energy develops (see Figure 1 of [34]). Hence after the initial instability the system evolution is broadly similar to those where a complex rotational braiding flow is applied. A similar finding occurs for the localised single vortex driver after the initial kink instability [35]. This suggests the nature of the photospheric motions are not important for loop heating, in contrast to other results [48] that will be discussed in Section 2.4.

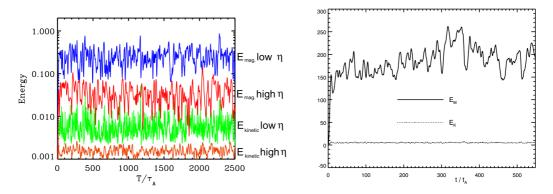
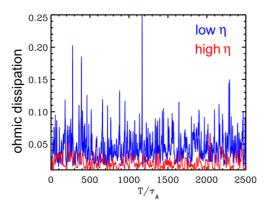


Figure 5: Variation of total magnetic and kinetic energies in time in particular simulation runs of continually driven systems: [36] (left) and [32, 33] (right). In both cases time is measured in units of the Alfvén crossing time along the loop. Shown in the figures and common to all simulations of Section 2.2 is a intermittent fluctuation of the quantities about average values, with a dominance of magnetic energy over kinetic energy. Left: image adapted from [36]. Right: image reproduced with permission from [33], copyright AAS.

Dissipation in these systems has a similar character, with both ohmic and viscous dissipation having a bursty, intermittent nature, illustrated for some example runs in Figure 6. Poynting flux into the volume and dissipation are coupled only on long time periods, with the de-correlation being particularly noticeable during strong heating events [32]. The average heating rate is found to increase and the fluctuations to become increasingly fast as the magnetic Reynolds number increases [36] (see also Figure 12 of [33], for example). The dependency on resistivity, η , was examined systematically first by Longcope & Sudan [29] and then over a wider range of η given the newly available increased computing power by Ng et al. [36]. The Ng et al. [36] results show that the $\eta^{-1/3}$ dependency found by Longcope & Sudan [29] begins to turn over as η is decreased. The behaviour over further orders of magnitude in η is far from clear but the data clearly warn against extrapolating the few available points to solar parameters.



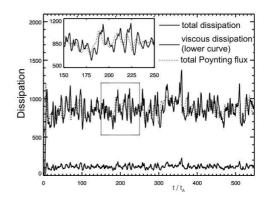


Figure 6: Dissipation shows a bursty, intermittent character in continually driven systems. Left: The level of dissipation increases with decreasing magnetic Reynolds number seen in the example of [36] (image adapted from [36]). Right: Dissipation and Poynting flux balance only on long timescales but are decoupled on short periods, seen in the example of [32, 33] (image adapted from [32]).

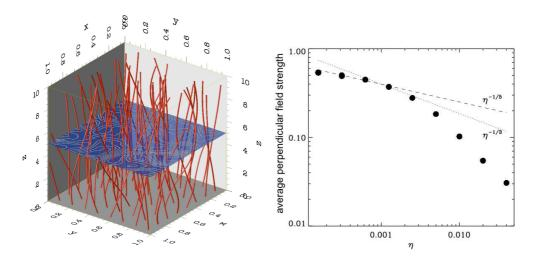


Figure 7: Left: example magnetic field lines in a continually driven system of Rappazzo et al. [32, 33] showing low levels of braiding in the statistically steady state. Image reproduced with permission from [33], copyright AAS. Right: A detailed examination of B_{\perp} in Ng et al.'s reduced MHD simulations [36] shows an increase of average B_{\perp} as η decreases. Image adapted from [36].

Linked with both the dissipation and the magnetic energy is the magnetic field structure. Rappazzo et al. [32, 33] find that the magnetic field stays close to uniform, with typical inclinations being of the order 2° , illustrated in Figure 7 (left). While [32, 33] do not detail how the structure depends on magnetic Reynolds number, Ng et al. [36] examines this more closely, showing how the average perpendicular field strength B_{\perp} increases with decreasing η (Figure 7, right). Note that a basic assumption of RMHD is that B_{\perp} is an order of magnitude less than B_z under the evolution and hence the findings lead one to ask whether this trend would also occur in a full 3D MHD evolution.

The current structure in these continually driven systems [29, 30, 31, 32, 33, 36, 37] are broadly similar, with long thin current layers extending vertically through much of the domain (see Figure 6 of [31], Figure 18 of [33], Figure 1 of [36], for example). Part of this structure is enforced by the basic RMHD assumption where only the vertical current component is retained. In the continually driven shearing simulations of Galsgaard & Nordlund [22] a much more fragmented and intermittent structure is found (Figure 3 here, see also Figure 9 of [22]). However, although a fully 3D MHD evolution was considered in [22], the initial plasma beta was set at $\beta = 0.5$ and the energy equation neglected conduction and radiation so that a high- β state developed. Note that in the reduced MHD simulations the lack of an energy equation essentially implies $\beta = 0$ throughout. The only fully 3D MHD long duration simulations including conduction and radiation to date seem to be those of Dahlburg et al. [37]. These authors are the first to show that the internal energy also has an intermittent, statistically steady nature. The temperature of their coronal loops corresponds closely to the current structure and is found to be highly spatially structured, giving a multi-thermal loop where only a fraction of the volume shows significant heating at any one time. Dahlburg et al. [37] find "the dynamics of this problem are well represented by RMHD" with low average twist (maximum 3°) and an almost incompressible flow, although a detailed comparison is not made in the letter.

2.3 Formation of Discontinuities

A third class of simulations consider the Parker problem, i.e. whether or not truly singular currents form under an ideal MHD evolution where a topologically simple magnetic field is subjected to complex boundary motions. Several of the sequences of boundary shear works discussed in Section 2.1 address this question. In summary, successive application of low amplitude shear current layer thickness exponentially decreases with number of shears (i.e. finite thickness currents) [18, 18, 20]. For sufficiently strong shear behaviour

is consistent with the formation of singular current sheets, up to the numerical resolution available [21].

Moving to the more general class of simulation, Craig & Sneyd [42] presented a series of simulations where a wide variety of boundary motions were applied to a uniform magnetic field on a unit cube, again using the magnetofrictional relaxation technique [25, 21]. In almost all cases considered smooth, well-resolved, large-scale currents are obtained. For example, following a particular combination of localised shear and compression the current structure shown in Figure 8 (left) is found. Only for one type of footpoint motion do the authors find behaviour that is consistent with the formation of a singular current sheet, this being where footpoint displacements involve the side-boundaries of the loop. Under these circumstances and given motions of sufficient amplitude, the maximum current in a relaxed equilibrium increases with grid resolution (to the maximum available resolution of 81³), as illustrated in Figure 8 (right). This finding is in common with Longbottom et al. [21]. However the authors point out that the types of motions employed in both works are not those originally envisaged under the Parker problem (i.e. they are not complex motions internal to a loop but rather involve the entire loop).

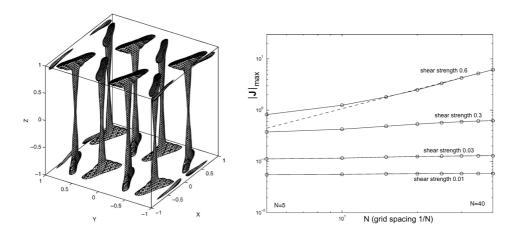


Figure 8: Left: Isosurfaces of current density in an equilibrium state following localised boundary motions of shear and compression applied to a uniform field and obtained under a magnetofrictional relaxation. A wide variety of boundary motions considered also resulted in smooth equilibria [42]. Right: Only for footpoint motions also involving the side boundaries was behaviour consistent with singular current sheet formation – illustrated by the power-law growth for sufficiently strong shear. Images reproduced with permission from [42].

With this in mind a series of works by the group in Dundee have examined the nature of currents in magnetic fields that are braided [43, 44, 45, 46, 47, 48, 49]. The idea differs

from previous simulations in that, rather than starting with a uniform magnetic field and braiding it through boundary motions, the initial configuration is already braided [43] (chosen as an analytical expression where some magnetic field lines have a pigtail braid topology while more generally field lines show a complex continuum of connectivities). Overall the configuration has no helicity, being built up from an equal number of positive and negative twists. The energy required to create the field is low, with about 3% magnetic energy in excess of potential [43]. The field line mapping of the braided magnetic field shows small scales, with the thickness of the QSLs in the field decreasing exponentially with braid complexity [44], mirroring the finding of van Ballegooijen [18] for the multiple shear case. The authors then ask whether the pigtail braid configuration can be ideally deformed to a force-free state: if so then the space of force-free fields is surely not as restricted as Parker envisaged. To carry out this evolution the aforementioned magnetofrictional relaxation scheme was employed [43]. The ideal relaxation is able to bring the braided field to a near force-free state where current structures show only large scales (Figure 9, left-most image). However, numerical difficulties with the scheme [27] prevent relaxation to perfectly force-free (a state that anyway can only be asymptotically reached in a simulation). A more recent detailed investigation has suggested that as the force-free state is approached even more closely, the current structure would develop small scales, with the thickness of current layers having the same width as the QSLs of the field and so exponentially decreasing with level of braiding [49]. Again this mirrors the finding of van Ballegooijen [19]. In any case, in a resistive MHD simulation the current is found to collapse and reconnection to begin across the resulting layers [45]. The subsequent evolution of the field, together with other similar simulations, is the subject of the next section.

2.4 Initially braided fields

The near-force-free magnetic field with a pigtail braid topology described in the previous section has been used as an initial condition for a resistive MHD evolution [45, 46]. At the magnetic Reynolds numbers presently numerically accessible the current system quickly intensifies and collapses to form two thin current layers [45]. These layers then fragment and a complex network of current layers with a volume filling effect is formed (Figure 9). Magnetic reconnection taking place across these layers allows the magnetic field to simplify and form an equilibrium state consisting of two unlinked flux tubes of opposite twist, associated with large scale currents (Figure 9, right-most image) [46]. Thus, although helicity is very well conserved, relaxation is not to the expected Taylor

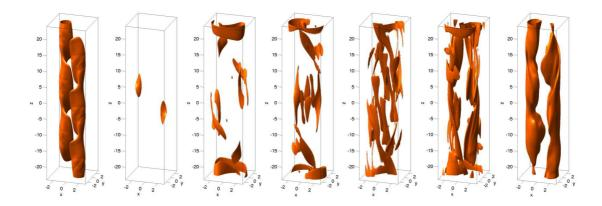


Figure 9: Isosurfaces of current in time (t = 0, 15, 27, 35, 50, 140, 290) during a resistive MHD relaxation of a braided magnetic field. After [46].

state, limiting the magnetic energy release [47]. The braiding is found to be associated with a homogeneous loop heating [48]. By contrast a comparison case of a more coherent braided field, constructed from twisting motions of only one sign, was examined and found to lead to more localised but stronger heating [48]. These contrasting cases, illustrated in Figure 10 suggest that the nature of photospheric motions will indeed have a strong impact on heating via magnetic braiding.

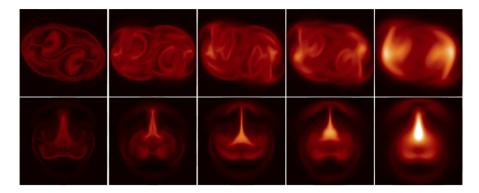


Figure 10: Loop heating in time (t=40,80,120,180,350) for two contrasting resistive relaxations of braided magnetic fields. The upper panel shows the homogeoneous heating of a complex braided field and the lower panel the more localised intense heating for a more coherently braided field. Field line averaged temperature along the loop is shown in the loop mid-plane. After [48].

In a broadly similar spirit Rappazzo & Parker [50] present a series of simulations following the resistive reduced MHD evolution of braided magnetic fields. The fields, not themselves in equilibrium, are constructed by superimposing a perpendicular field component made up of large scale Fourier modes to the background uniform field, so creating a braided loop (taken with aspect ratio 1:10). The loop evolution was found to depend on the ratio, b_0/B_0 , between the root mean square amplitude of the initial perpendicular field and the background field. For $b_0/B_0 \gtrsim 4\%$ the system develops current layers and a resistive turbulent decay ensues, with some but not all of the free magnetic energy being dissipated (see Figure 11). The authors suggested that the ratio b_0/B_0 required before a violent decay could take place depends on the loop aspect ratio, as $\sim l/3.5L$ (where l is the horizontal and L the vertical loop dimension). Next Rappazzo & Parker [50] consider whether the current layers forming in the early resistive RMHD evolution would be singular in an ideal evolution. For this the same RMHD scheme was deployed, taking a high resolution and only numerical dissipation. The analyticity strip method [51] was applied to examine whether the nature of the current evolution is indicative of a singularity, but no conclusion could be drawn, with the method itself failing. Nevertheless the early evolution shows strong and highly localised current enhancements, as shown in Figure 11 (right).

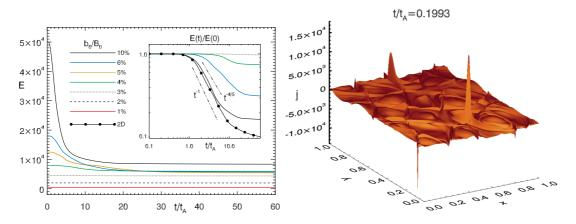


Figure 11: (Left) Total magnetic energy in time for braided non-equilibrium magnetic fields under a resistive reduced MHD evolution. The ratio b_0/B_0 relates to the initial energy of the perpendicular field component. For sufficiently high b_0/B_0 a turbulent decay releases much of the free energy. (Right) Current j_z after $t/t_A = 0.1993$ in the ideal reduced MHD simulation ($4096^2 \times 2048$ resolution), taken in the mid-plane of the loop. Strong and localised current layers form but it cannot be established whether or not they are singular. Images reproduced with permission from [50], copyright AAS.

3 Conclusions and Future Directions

The emerging consensus from flux braiding experiments is that thin but non-singular current layers form as coronal loops are subjected to braiding motions and that the width of these layers decreases exponentially in time. With photospheric motions continually but slowly braiding the coronal volume dissipation is an inevitable consequence. In simulations where systems have a finite resistivity and are subjected to footpoint motions over a long period of time statistically steady states are reached where dissipation and magnetic energy fluctuate strongly in time about an average level. Although the Poynting flux into the corona must balance over a long time (with short-term decoupling present in simulations) the flux is itself dependent on the state of the coronal field. How exactly heating depends on the nature of the photospheric motions and on the coronal resistivity is not well understood.

A number of ideas arise for future attacks on the braiding problem. One is to update the simulation approach to the singularity question of Parker using improved computational techniques. For example, the magnetofrictional relaxation scheme, previously known to have numerical inaccuracies, has been significantly improved and at the same time parallelised so that simulations with an order of magnitude higher resolution are possible [28].

For the case where loops are continually subjected to boundary motions a more detailed examination with systematic simulation setup is required to determine what exactly are the important factors in determining the level and nature of the loop heating. Before tackling this with a reduced MHD approach a careful comparison of reduced MHD with fully 3D MHD could perhaps be fruitful.

In a move towards increased realism a basic question is how the corona can be braided when a realistic loop is modelled. Part of this is to take a representative stratified atmosphere, with important initial advances recently presented by van Ballegooijen et al. [52]. Additionally one should recall that the real corona is full of topological structure so that how coronal fields are braided when the magnetic carpet is included, i.e. simulations addressing the coronal tectonics hypothesis [9], is another task for the near future. Similarly along these lines the ever-increasing computing power should allow a better resolution of large-scale simulations (e.g. [14, 15, 16, 17]) so that their relation to braiding and coronal tectonics can be more completely established.

Acknowledgment

Helpful discussions with Peter Cargill, Jim Klimchuk, and the Dundee MHD group and financial support from STFC (ST/K000993/1) are all gratefully acknowledged.

References

- [1] Parker EN. 1972. Topological Dissipation and the Small-Scale Fields in Turbulent Gases. Astrophys. J. 174 499-510. doi: 10.1086/151512
- [2] Parker EN. 1988. Nanoflares and the solar X-ray corona Astrophys. J. 330 474-479. doi: 10.1086/166485
- [3] Parker EN. 1994. Spontaneous Current Sheets in Magnetic Fields: With Applications to Stellar X-Rays. *International Series in Astronomy and Astrophysics*, Oxford University Press, Oxford.
- [4] Cirtain JW, Golub L, Winebarger AR, De Pontieu B, Kobayashi K, Moore RL, Walsh RW, Korreck KE, Weber M, McCauley P, Title A, Kuzin S, DeForest CE. 2013. Energy release in the solar corona from spatially resolved magnetic braids. Nature 493 501-503. doi: 10.1038/nature11772
- [5] Cargill P. 2013. Solar physics: Towards ever smaller length scales. Nature 493 485-486. doi: 10.1038/493485a
- [6] Thalmann JK, Tiwari SK, Wiegelmann T. 2014. Force-free field modeling of twist and braiding-induced magnetic energy in an active region corona. Astrophys. J. 780 id. 102 (8pp). doi: 10.1088/0004-637X/780/1/102
- [7] Priest ER. 2014. Magnetohydrodynamics of the Sun. Cambridge University Press Cambridge.
- [8] Parnell CE. 2015. The importance of magnetic topology for coronal heating. (An invited review to appear in this volume.)
- [9] Priest ER, Heyvaerts, JF, Title AM. 2002. A flux-tube tectonics model for solar coronal heating driven by the magnetic carpet. Astrophys. J. 576 533-551. doi: 10.1086/341539

- [10] Mellow C, Gerrard CL, Galsgaard K, Hood AW, Priest ER. 2005. Numerical simulations of the flux tube tectonics model for coronal heating. Solar Phys. 227 39-60. doi: 10.1007/s11207-005-1713-2
- [11] De Moortel I, Galsgaard K. 2006. Numerical modelling of 3D reconnection due to rotational footpoint motions. Astron. Astrophys. 451 1101-1115. doi: 10.1051/0004-6361:20054587
- [12] De Moortel I, Galsgaard K. 2006. Numerical modelling of 3D reconnection II. Comparison between rotational and spinning footpoint motions. Astron. Astrophys. 459 627-639. doi: 10.1051/0004-6361:20065716
- [13] Wilmot-Smith AL, De Moortel I. 2007. Magnetic reconnection in flux tubes undergoing spinning footpoint motions. Astron. Astrophys. 473 615-623. doi: 10.1051/0004-6361:20077455
- [14] Gudiksen BV, Nordlund Å. 2002. Bulk heating and slender magnetic loops in the solar corona. Astrophys. J. 572 L113-L116. doi: 10.1086/341600
- [15] Peter H, Gudiksen BV, Nordlund Å. 2004. Coronal heating through braiding of magnetic field lines. Astrophys. J. 617 L85-L88. doi: 10.1086/427168
- [16] Gudiksen BV, Nordlund A. 2005. An ab initio approach to the coronal heating problem. Astrophys. J. 618 1020-1030. doi: 10.1086/426063
- [17] Gudiksen BV, Nordlund Å. 2005. An ab initio approach to solar coronal loops. Astrophys. J. 618 1031-1038. doi: 10.1086/426064
- [18] van Ballegooijen AA. 1988a. Force Free Fields and Coronal Heating Part 1. The Formation of Current Sheets. Geophys. Astrophys. Fluid Dyn. 41 181-211. doi: 10.1080/03091928808208850
- [19] van Ballegooijen AA. 1988b. Magnetic Fine Structure of Solar Coronal Loops. Solar and stellar coronal structure and dynamics; Proceedings of the Ninth Sacramento Peak Summer Symposium, Sunspot, NM. p. 115-124.
- [20] Mikić Z, Schnack DD, van Hoven G. 1989. Creation of Current Filaments in the Solar Corona. Astrophys. J. 338 1148-1157. doi:10.1086/167265
- [21] Longbottom AW, Rickard GJ, Craig IJD, Sneyd AD. 1998. Magnetic Flux Braiding: Force-Free Equilibria and Current Sheets. Astrophys. J. 500 471-482. doi: 10.1086/305694

- [22] Galsgaard K, Nordlund Å. 1996. Heating and activity of the solar corona 1. Boundary shearing of an initially homogeneous magnetic field. J. Geophys. Res. 101 (A6) 13445-13460. doi: 10.1029/96JA00428
- [23] Bowness R, Hood AW, Parnell CE. 2013. Coronal heating and nanoflares: current sheet formation and heating. Astron. Astrophys. 560 A89. doi: 10.1051/0004-6361/201116652
- [24] Titov VS, Hornig G, Démoulin P. 2002. Theory of magnetic connectivity in the solar corona. J. Geophys. Res. 107 A8 id. 1164. doi: 10.1029/2001JA000278
- [25] Craig IJD, Sneyd AD. 1986. A dynamic relaxation technique for determining the structure and stability of coronal magnetic fields. Astrophys. J. 311 451-459. doi: 10.1086/164785
- [26] Ali F, Sneyd A. 2001. Magnetic equilibria resulting from a helically symmetric kink instability. Geophys. Astrophys. Fluid Dyn. 94 (3) 221-248. doi: 10.1080/03091920108203408
- [27] Pontin DI, Hornig G, Wilmot-Smith AL, Craig IJD. 2009. Lagrangian Relaxation Schemes for Calculating Force-free Magnetic Fields, and Their Limitations. Astrophys. J. 700 (2) 1449-1455. doi: 10.1088/0004-637X/700/2/1449
- [28] Candelaresi S, Pontin D, Hornig G. 2014. Mimetic Methods for Lagrangian Relaxation of Magnetic Fields. SIAM Journal on Scientific Computing, in press.
- [29] Longcope DW, Sudan RN. 1994. Evolution and Statistics of Current Sheets in Coronal Magnetic Loops. Astrophys. J. 437 491–504. doi: 10.1086/175013
- [30] Hendrix DL, van Hoven G. 1996. Magnetohydrodynamic Turbulence and Implications for Solar Coronal Heating. *Astrophys. J.* **467** 887-893. doi: 10.1086/177663
- [31] Gomez DO, Dmitruk PA, Milano LJ. 2000. Recent Theoretical Results on Coronal Heating. Solar Phys. 195 299–318. doi: 10.1023/A:1005283923956
- [32] Rappazzo AF, Velli M, Einaudi G, Dahlburg RB. 2007. Coronal Heating, Weak MHD Turbulence, and Scaling Laws. Astrophys. J. 657 L47-L51. doi: 10.1086/512975
- [33] Rappazzo AF, Velli M, Einaudi G, Dahlburg RB. 2008. Nonlinear Dynamics of the Parker Scenario for Coronal Heating. Astrophys. J. 677 1348-1366. doi: 10.1086/528786

- [34] Rappazzo AF, Velli M, Einaudi G. 2010. Shear Photospheric Forcing and the Origin of Turbulence in Coronal Loops. Astrophys. J. 722 65-78. doi: 10.1088/0004-637X/722/1/65
- [35] Rappazzo AF, Velli M, Einaudi G. 2013. Field Lines Twisting in a Noisy Corona: Implications for Energy Storage and Release, and Initiation of Solar Eruptions. Astrophys. J. 771 (2) id. 76, 14 pp. doi: 10.1088/0004-637X/771/2/76
- [36] Ng CS, Lin L, Bhattacharjee A. 2012. High-Lundquist Number Scaling in Three-dimensional Simulations of Parker's Model of Coronal Heating Astrophys. J. 747 2 id. 109 10pp. doi: 10.1088/0004-637X/747/2/109
- [37] Dahlburg RB, Einaudi G, Rappazzo AF, Velli M. 2012. Turbulent coronal heating mechanisms: coupling of dynamics and thermodynamics. A&A 544 L20. doi: 10.1051/0004-6361/201219752
- [38] Stauss HR. 1976. Nonlinear, three-dimensional magnetohydrodynamics of noncircular tokamaks. *Phys. Fluids* **19** 134-140. doi: 10.1063/1.861310
- [39] Stauss HR. 1977. Dynamics of high beta Tokamaks. Phys. Fluids 20 1354-1360. doi: 10.1063/1.862018
- [40] Rosenbluth MN, Monticello DA, Strauss HR, White RB. 1976. Numerical studies of nonlinear evolution of kink modes in Tokamaks. *Phys. Fluids* 19 1987-1996. doi: 10.1063/1.861430
- [41] Longcope DW. 1993. Theoretical studies of magnetohydrodynamic equilibria and dynamics of a solar coronal loop. Ph.D. Thesis, Cornell University, Ithaca NY.
- [42] Craig IJD, Sneyd AD. 2005. The Parker Problem and the Theory of Coronal Heating. Solar Phys. 232 41-62. doi: 10.1007/s11207-005-1582-8
- [43] Wilmot-Smith AL, Hornig G, Pontin DI. 2009. Magnetic Braiding and Parallel Electric Fields, Astrophys. J. 696 1339-1347 doi: 10.1088/0004-637X/696/2/1339
- [44] Wilmot-Smith AL, Hornig G, Pontin DI. 2009. Magnetic Braiding and Quasi-Separatrix Layers Astrophys. J. 704 1288-1295. doi: 10.1088/0004-637X/704/2/1288
- [45] Wilmot-Smith AL, Pontin DI, Hornig G. 2010. Dynamics of braided coronal loops
 I. Onset of magnetic reconnection. Astron. Astrophys. 516 A5. doi: 10.1051/0004-6361/201014041

- [46] Pontin DI, Wilmot-Smith AL, Hornig G, Galsgaard K. 2010. Dynamics of braided coronal loops - II. Cascade to multiple small-scale reconnection events. Astron. Astrophys. 525 A57. doi: 10.1051/0004-6361/201014544
- [47] Yeates AR, Hornig G, Wilmot-Smith AL. 2010. Topological Constraints on Magnetic Relaxation. Phys. Rev. Letters 105 (8) 085002. doi: 10.1103/Phys-RevLett.105.085002
- [48] Wilmot-Smith AL, Pontin DI, Yeates AR, Hornig G. 2011. Heating of braided coronal loops. Astron. Astrophys. 536 A67. doi: 10.1051/0004-6361/201117942
- [49] Pontin DI, On the degree of field line braiding in coronal loops, in preparation
- [50] Rappazzo AF, Parker EN. 2013. Current Sheets Formation in Tangled Coronal Magnetic Fields. Astrophys. J. 773: L2 (6pp). doi: 10.1088/2041-8205/773/1/L2
- [51] Sulem C, Sulem P-L, Frisch, H. 1983. Tracing complex singularities with spectral methods J. Comput. Phys. 50 138-161. doi: 10.1016/0021-9991(83)90045-1
- [52] van Ballegooijen AA, Asgari-Targhi M, Berger MA. 2014. On the Relationship Between Photospheric Footpoint Motions and Coronal Heating in Solar Active Regions. Astrophys. J. 787 1 id. 87, 14pp. doi: 10.1088/0004-637X/787/1/87